# Spectral Amplitude-Coding Optical CDMA System Using Mach–Zehnder Interferometers

Cheing-Hong Lin, Jingshown Wu, *Fellow, IEEE*, Hen-Wai Tsao, *Member, IEEE*, and Chun-Liang Yang

***Abstract*—In this paper, we propose a family of newly constructed codes to suppress the phase-induced intensity noise (PIIN) in spectral amplitude-coding (SAC) optical code division multiple access (OCDMA) systems. These new codes are derived from modified prime codes and their cross-correlation is not larger than one. We also present a novel SAC-OCDMA system employing the new codes together with Mach–Zehnder interferometers to eliminate the multi-user interference (MUI). Compared with the systems employing modified quadratic congruence codes (MQC codes), numerical results verify that our proposed system can more effectively suppress the PIIN and eliminate MUI. Hence, the number of simultaneously users and total transmission rate increases significantly.**

***Index Terms*—Optical code-division multiple access (OCDMA), spectral amplitude coding (SAC), modified prime codes, multi-user interference (MUI), Mach–Zehnder interferometer.**

## I. Introduction

THE optical code-division multiple-access (OCDMA) system has been investigated for about two decades and received a lot of attention. The OCDMA system has the advantage of providing multiple users to access the same bandwidth simultaneously without employing high-speed electronic data processing circuits that are necessary in the time-division multiple-access (TDMA) networks. Further, it also has the advantage of providing high-level security during transmission.

Conventional OCDMA systems, depending on the requirement of time synchronization, can be classified into synchronous and asynchronous systems. In general, the spreading sequences used in synchronous systems are modified prime codes and perfect difference codes [1]–[3] while the spreading sequences used in asynchronous systems are optical orthogonal codes (OOCs) [4]–[7]. The code sizes of modified prime codes and perfect difference codes are much larger than that of OOCs having the same code length. On the contrary, the OOCs have better auto- and cross-correlation properties than the modified prime sequence codes so that they are suitable for asynchronous systems.

In recent years, spectral amplitude-coding (SAC) OCDMA system attracts more attention since the multi-user interference (MUI) can be completely eliminated by spectral coding. Code sequences with fixed in-phase cross-correlation such as Hadamard codes have been used to remove the MUI [7], [8]. However, since the value of the in-phase cross-correlation between code sequences is large, the phase-induced intensity noise (PIIN) severely degrades the system performance. In view of this disadvantage, Zhou *et al.* [9] and Wei *et al.* [10] used codes with a fixed in-phase cross-correlation exactly equal to one for suppressing the effect of PIIN. However, since the in-phase cross-correlation of these codes is always one, the PIIN induced in the system employing these codes is still significant, thus limiting the system performance for further improvement. In this paper, we relax this constraint and construct new codes with in-phase cross-correlation not larger than one and furthermore propose a system architecture using such codes together with Mach–Zehnder interferometers to eliminate MUI to further suppress PIIN.

The rest of this paper is organized as following. The family of newly constructed codes, named partial modified prime codes (PMP), is described in Section II. Section III presents the proposed system architecture in details. The analytic results of system performance are presented in Section IV. The numerical and simulation results are shown in Section V. Finally, we give the conclusion in Section VI.

## II. Partial Modified Prime Codes

The prime codes are a set of code sequences with code length $L = p^2$ derived from prime sequences, where $p$ is a prime number [1]. Elements of a prime sequence can be obtained by multiplying each element in the Galois field $\mathrm{GF}(p) = \{0, 1, \ldots, p-1\}$ by a preset number chosen from $\mathrm{GF}(p)$. Hence, there are $p$ prime sequences. We then map these prime sequences to binary code sequences to form the prime codes. For example, the prime sequence $S_x = (s_{x,0}, s_{x,1}, \ldots, s_{x,j}, \ldots, s_{x,(p-1)})$ is mapped to the code sequence $C_x = (c_{x,0}, c_{x,1}, \ldots, c_{x,i}, \ldots, c_{x,(p^2-1)})$ according to

$$c_{x,i} = \begin{cases} 1, & \text{for } i = s_{x,j} + jp, \quad j = 0, 1, \ldots, p-1 \\ 0, & \text{otherwise.} \end{cases} \tag{1}$$

On the other hand, the modified prime codes, which are used in synchronous systems, are time-shift versions of the prime codes [2]. To construct the modified prime codes, we take a prime sequence $S_x$ and rotate it by $p-1$ times to create new prime sequences $S_{x,r} = (s_{x,r,0}, s_{x,r,1}, \ldots, s_{x,r,j}, \ldots, s_{x,r,(p-1)})$, where $r$ refers to the number of left-rotations. Likewise, a mapped code sequence $C_{x,r} = (c_{x,r,0}, c_{x,r,1}, \ldots, c_{x,r,i}, \ldots, c_{x,r,(p^2-1)})$ can be obtained according to

$$c_{x,r,i} = \begin{cases} 1, & \text{for } i = s_{x,r,j} + jp, \quad j = 0, 1, \ldots, p-1 \\ 0, & \text{otherwise.} \end{cases} \tag{2}$$

Manuscript received November 24, 2003; revised July 12, 2004. Part of this work was supported by Nation Science Council and the Ministry of Education, Taiwan, R.O.C. under Grant NSC 91-2213-E-002-106 and Grant 89E-FA06-2-4-7.

C.-H. Lin, J. Wu, and H.-W. Tsao are with the Department of Electrical Engineering and Graduate Institute of Communication Engineering, National Taiwan University, Taipei, Taiwan 10617, R.O.C.

C.-L. Yang is with the Department of Electrical Engineering, Tamkang University, Taipei, Taiwan 10617, R.O.C.

Digital Object Identifier 10.1109/JLT.2005.844205

TABLE I
EXAMPLE OF THE MODIFIED PRIME CODES FOR GF(5)

| Group $x$ | $i$ 01234 | Sequence | Code Sequence | | | | |
|---|---|---|---|---|---|---|---|
| 0 | 00000 | $S_{0,0}$ | $C_{0,0}$= 10000 | 10000 | 10000 | 10000 | 10000 |
| | 44444 | $S_{0,1}$ | $C_{0,1}$= 00001 | 00001 | 00001 | 00001 | 00001 |
| | 33333 | $S_{0,2}$ | $C_{0,2}$= 00010 | 00010 | 00010 | 00010 | 00010 |
| | 22222 | $S_{0,3}$ | $C_{0,3}$= 00100 | 00100 | 00100 | 00100 | 00100 |
| | 11111 | $S_{0,4}$ | $C_{0,4}$= 01000 | 01000 | 01000 | 01000 | 01000 |
| 1 | 01234 | $S_{1,0}$ | $C_{1,0}$= 10000 | 01000 | 00100 | 00010 | 00001 |
| | 12340 | $S_{1,1}$ | $C_{1,1}$= 01000 | 00100 | 00010 | 00001 | 10000 |
| | 23401 | $S_{1,2}$ | $C_{1,2}$= 00100 | 00010 | 00001 | 10000 | 01000 |
| | 34012 | $S_{1,3}$ | $C_{1,3}$= 00010 | 00001 | 10000 | 01000 | 00100 |
| | 40123 | $S_{1,4}$ | $C_{1,4}$= 00001 | 10000 | 01000 | 00100 | 00010 |
| 2 | 02413 | $S_{2,0}$ | $C_{2,0}$= 10000 | 00100 | 00001 | 01000 | 00010 |
| | 24130 | $S_{2,1}$ | $C_{2,1}$= 00100 | 00001 | 01000 | 00010 | 10000 |
| | 41302 | $S_{2,2}$ | $C_{2,2}$= 00001 | 01000 | 00010 | 10000 | 00100 |
| | 13024 | $S_{2,3}$ | $C_{2,3}$= 01000 | 00010 | 10000 | 00100 | 00001 |
| | 30241 | $S_{2,4}$ | $C_{2,4}$= 00010 | 10000 | 00100 | 00001 | 01000 |
| 3 | 03142 | $S_{3,0}$ | $C_{3,0}$= 10000 | 00010 | 01000 | 00001 | 00100 |
| | 31420 | $S_{3,1}$ | $C_{3,1}$= 00010 | 01000 | 00001 | 00100 | 10000 |
| | 14203 | $S_{3,2}$ | $C_{3,2}$= 01000 | 00001 | 00100 | 10000 | 00010 |
| | 42031 | $S_{3,3}$ | $C_{3,3}$= 00001 | 00100 | 10000 | 00010 | 01000 |
| | 20314 | $S_{3,4}$ | $C_{3,4}$= 00100 | 10000 | 00010 | 01000 | 00001 |
| 4 | 04321 | $S_{4,0}$ | $C_{4,0}$= 10000 | 00001 | 00010 | 00100 | 01000 |
| | 43210 | $S_{4,1}$ | $C_{4,1}$= 00001 | 00010 | 00100 | 01000 | 10000 |
| | 32104 | $S_{4,2}$ | $C_{4,2}$= 00010 | 00100 | 01000 | 10000 | 00001 |
| | 21043 | $S_{4,3}$ | $C_{4,3}$= 00100 | 01000 | 10000 | 00001 | 00010 |
| | 10432 | $S_{4,4}$ | $C_{4,4}$= 01000 | 10000 | 00001 | 00010 | 00100 |

Each prime code sequence can generate $p-1$ new code sequences to form a code group. Hence, the modified prime codes can be divided into $p$ groups and the total number of codes is $p^2$. An example of the modified prime codes derived from GF(5) is shown in Table I. Under synchronized condition, the cross-correlation between the $x$th and $y$th modified prime codes is

$$\Gamma_{x,y}=\begin{cases}p, & x=y\\ 0, & x \text{ and } y \text{ are in the same group}\\ 1, & x \text{ and } y \text{ are in different groups.}\end{cases} \tag{3}$$

According to (3), the cross-correlation between the $x$th and $y$th codes is zero when they belong to the same group, or one otherwise. Since the cross-correlation of the modified prime codes is never larger than one, the modified prime codes are superior to the modified quadratic congruence (MQC) codes [10], whose cross-correlation is equal to one, for suppressing PIIN. However, the cross-correlation of the modified prime codes is also equal to one in most situations, i.e., the situation that the codes are in different groups. Hence, the improvement is insignificant.

In order to further suppress the PIIN, we relax the constraint of the cross-correlation of the modified prime codes and propose the PMP codes in this paper to reduce the beating rate between the code sequences. The PMP codes are divided versions of the modified prime codes. Each of the modified prime sequences can be used to generate several new sequences. This means that the modified prime sequence $S_{x,r}$ constructed from GF($p$) can be divided to form $M$ new prime sequences $S_{x,r,m}=(s_{x,r,m,0},s_{x,r,m,1},\ldots,s_{x,r,m,j},\ldots,s_{x,r,m,(p-1)})$, where $M$ is a factor of $(p-1)$ and $m\in\{0,\ldots,M-1\}$.

For instance, if $M=2$, the modified prime sequence $S_{x,r}$ can be separated as $S_{x,r,0}=(s_{x,r,0,0}=s_{x,r,0},s_{x,r,0,1}=\mathrm{X},\ldots,s_{x,r,0,x}=\mathrm{X},\ldots,s_{x,r,0,(p-2)}=s_{x,r,(p-2)},s_{x,r,0,(p-1)}=\mathrm{X})$, and $S_{x,r,1}=(s_{x,r,1,0}=\mathrm{X},s_{x,r,1,1}=s_{x,r,1},\ldots,s_{x,r,1,x}=\mathrm{X},\ldots,s_{x,r,1,(p-2)}=\mathrm{X},\ s_{x,r,1,(p-1)}=s_{x,r,(p-1)})$, wherein X = null. The mapped code sequences $C_{x,r,m}=(c_{x,r,m,0},c_{x,r,m,1},\ldots,c_{x,r,m,i},\ldots,c_{x,r,m,(p^2-1)})$ can be obtained according to (4) shown at the bottom of the page.

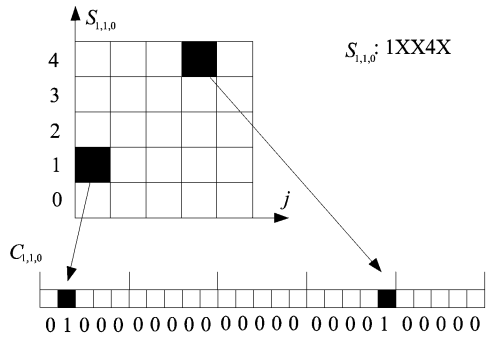


Fig. 1. An exemplary procedure for generating (0, 1) sequence $C_{x,r,m}$ based on the partial modified prime sequence $S_{x,r,m}$.

By using this scheme, the size of each group of the modified prime codes is expanded $M$ times. The code size of the PMP codes is $Mp^2$ and the code weight is reduced to $(p-1)/M$. Therefore, the beating rate of any two PMP code sequences can be reduced as the value of the dividing factor $M$ is increased. The PIIN can be further suppressed by optimizing the value of $M$. An example of the PMP codes for GF(5) and $M=2$ is shown in Table II. Fig. 1 illustrates an exemplary procedure for generating (0, 1) sequence $C_{x,r,m}$ based on the partial modified prime sequence $S_{x,r,m}$.

$$c_{x,r,m,i}=\begin{cases}1, & \text{for } i=s_{x,r,m,j}+jp,\quad j=0,1,\ldots,p-1 \quad \text{and} \quad s_{x,r,m,j}\neq \mathrm{X}\\ 0, & \text{otherwise.}\end{cases} \tag{4}$$

TABLE II
EXAMPLE OF THE PARTIAL MODIFIED PRIME CODES FOR GF(5) AND $M = 2$

| Group $x$ | $i$ 01234 | Sequence | Code Sequence |
|---|---|---|---|
| 0 | X0X0X | $S_{0,0,0}$ | $C_{0,0,0}$= 00000 10000 00000 10000 00000 |
| | X4X4X | $S_{0,1,0}$ | $C_{0,1,0}$= 00000 00001 00000 00001 00000 |
| | X3X3X | $S_{0,2,0}$ | $C_{0,2,0}$= 00000 00010 00000 00010 00000 |
| | X2X2X | $S_{0,3,0}$ | $C_{0,3,0}$= 00000 00100 00000 00100 00000 |
| | X1X1X | $S_{0,4,0}$ | $C_{0,4,0}$= 00000 01000 00000 01000 00000 |
| | XX0X0 | $S_{0,0,1}$ | $C_{0,0,1}$= 00000 00000 10000 00000 10000 |
| | XX4X4 | $S_{0,1,1}$ | $C_{0,1,1}$= 00000 00000 00001 00000 00001 |
| | XX3X3 | $S_{0,2,1}$ | $C_{0,2,1}$= 00000 00000 00010 00000 00010 |
| | XX2X2 | $S_{0,3,1}$ | $C_{0,3,1}$= 00000 00000 00100 00000 00100 |
| | XX1X1 | $S_{0,4,1}$ | $C_{0,4,1}$= 00000 00000 01000 00000 01000 |
| 1 | 0XX3X | $S_{1,0,0}$ | $C_{1,0,0}$= 10000 00000 00000 00010 00000 |
| | 1XX4X | $S_{1,1,0}$ | $C_{1,1,0}$= 01000 00000 00000 00001 00000 |
| | 2XX0X | $S_{1,2,0}$ | $C_{1,2,0}$= 00100 00000 00000 10000 00000 |
| | 3XX1X | $S_{1,3,0}$ | $C_{1,3,0}$= 00010 00000 00000 01000 00000 |
| | 4XX2X | $S_{1,4,0}$ | $C_{1,4,0}$= 00001 00000 00000 00100 00000 |
| | XX2X4 | $S_{1,0,1}$ | $C_{1,0,1}$= 00000 00000 00100 00000 00001 |
| | XX3X0 | $S_{1,1,1}$ | $C_{1,1,1}$= 00000 00000 00010 00000 10000 |
| | XX4X1 | $S_{1,2,1}$ | $C_{1,2,1}$= 00000 00000 00001 00000 01000 |
| | XX0X2 | $S_{1,3,1}$ | $C_{1,3,1}$= 00000 00000 10000 00000 00100 |
| | XX1X3 | $S_{1,4,1}$ | $C_{1,4,1}$= 00000 00000 01000 00000 00010 |
| 2 | 0XX1X | $S_{2,0,0}$ | $C_{2,0,0}$= 10000 00000 00000 01000 00000 |
| | 2XX3X | $S_{2,1,0}$ | $C_{2,1,0}$= 00100 00000 00000 00010 00000 |
| | 4XX0X | $S_{2,2,0}$ | $C_{2,2,0}$= 00001 00000 00000 10000 00000 |
| | 1XX2X | $S_{2,3,0}$ | $C_{2,3,0}$= 01000 00000 00000 00100 00000 |
| | 3XX4X | $S_{2,4,0}$ | $C_{2,4,0}$= 00010 00000 00000 00001 00000 |
| | X2XX3 | $S_{2,0,1}$ | $C_{2,0,1}$= 00000 00100 00000 00000 00010 |
| | X4XX0 | $S_{2,1,1}$ | $C_{2,1,1}$= 00000 00001 00000 00000 10000 |
| | X1XX2 | $S_{2,2,1}$ | $C_{2,2,1}$= 00000 01000 00000 00000 00100 |
| | X3XX4 | $S_{2,3,1}$ | $C_{2,3,1}$= 00000 00010 00000 00000 00001 |
| | X0XX1 | $S_{2,4,1}$ | $C_{2,4,1}$= 00000 10000 00000 00000 01000 |
| 3 | 0X1XX | $S_{3,0,0}$ | $C_{3,0,0}$= 10000 00000 01000 00000 00000 |
| | 3X4XX | $S_{3,1,0}$ | $C_{3,1,0}$= 00010 00000 00001 00000 00000 |
| | 1X2XX | $S_{3,2,0}$ | $C_{3,2,0}$= 01000 00000 00100 00000 00000 |
| | 4X0XX | $S_{3,3,0}$ | $C_{3,3,0}$= 00001 00000 10000 00000 00000 |
| | 2X3XX | $S_{3,4,0}$ | $C_{3,4,0}$= 00100 00000 00010 00000 00000 |
| | X3XX2 | $S_{3,0,1}$ | $C_{3,0,1}$= 00000 00010 00000 00000 00100 |
| | X1XX0 | $S_{3,1,1}$ | $C_{3,1,1}$= 00000 01000 00000 00000 10000 |
| | X4XX3 | $S_{3,2,1}$ | $C_{3,2,1}$= 00000 00001 00000 00000 00010 |
| | X2XX1 | $S_{3,3,1}$ | $C_{3,3,1}$= 00000 00100 00000 00000 01000 |
| | X0XX4 | $S_{3,4,1}$ | $C_{3,4,1}$= 00000 10000 00000 00000 00001 |
| 4 | 0X3XX | $S_{4,0,0}$ | $C_{4,0,0}$= 10000 00000 00010 00000 00000 |
| | 4X2XX | $S_{4,1,0}$ | $C_{4,1,0}$= 00001 00000 00100 00000 00000 |
| | 3X1XX | $S_{4,2,0}$ | $C_{4,2,0}$= 00010 00000 01000 00000 00000 |
| | 2X0XX | $S_{4,3,0}$ | $C_{4,3,0}$= 00100 00000 10000 00000 00000 |
| | 1X4XX | $S_{4,4,0}$ | $C_{4,4,0}$= 01000 00000 00001 00000 00000 |
| | X4X2X | $S_{4,0,1}$ | $C_{4,0,1}$= 00000 00001 00000 00100 00000 |
| | X3X1X | $S_{4,1,1}$ | $C_{4,1,1}$= 00000 00010 00000 01000 00000 |
| | X2X0X | $S_{4,2,1}$ | $C_{4,2,1}$= 00000 00100 00000 10000 00000 |
| | X1X4X | $S_{4,3,1}$ | $C_{4,3,1}$= 00000 01000 00000 00001 00000 |
| | X0X3X | $S_{4,4,1}$ | $C_{4,4,1}$= 00000 10000 00000 00010 00000 |

Under synchronized condition, the cross-correlation between the $x$th and $y$th PMP codes is

$$\Gamma_{x,y} = \begin{cases} \dfrac{p-1}{M}, & x = y \\ 0, & x \text{ and } y \text{ are in the same group} \\ \leq 1, & x \text{ and } y \text{ are in different groups.} \end{cases} \tag{5}$$

Hence, if $C_n(g)$ denotes the $g$th element of the $n$th PMP code sequence, the relation between the code sequences can be written as:

$$\sum_{g=1}^{L} C_m(g) C_n(g) = \begin{cases} \dfrac{p-1}{M}, & m = n \\ \leq 1, & m \neq n \end{cases} \tag{6}$$

where $L$ is the code length, i.e., $L = p^2$.

## III. THE PROPOSED SYSTEM USING PMP CODES

Fig. 2 shows the schematic of the proposed system. The transmitter consists of a broadband source, a Mach–Zehnder interferometer and a spectral encoder. A high-power broadband superluminescent diode (SLD) or light-emitting diode (LED) can be employed as the broadband source. One arm of the Mach–Zehnder interferometer has a digital phase modulator inserted thereon. Thus, data can be modulated by phase-shift keying. Moreover, the spectral encoder will encode the modulated signal in spectrum according to a chosen PMP code sequence and then send the encoded signal to receivers through a star coupler.

The receiver consists of a spectral decoder, a Mach–Zehnder interferometer and a balanced detector. Therein, the balanced detector may consist of two avalanche photodiodes (APDs) or p-i-n photodiodes. Via the spectral decoder, the received signal

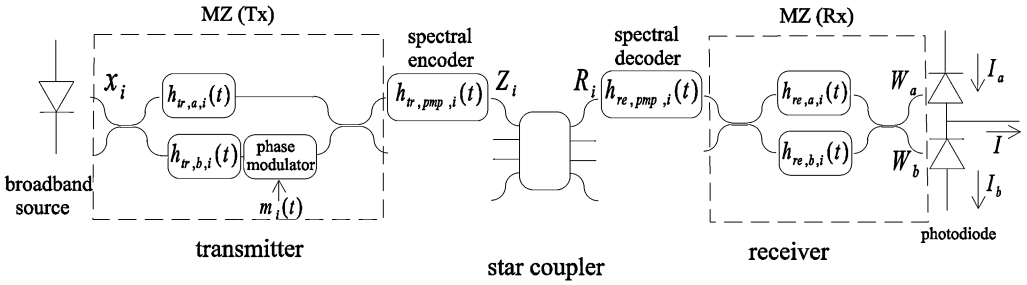


Fig. 2. OCDMA system using PMP codes.

can be decoded by using a matched code sequence and the unmatched spectral components will be filtered out. Then, through the Mach–Zehnder interferometer and balanced detector, the decoded signal is detected and the MUI from unmatched transmitters can be completely canceled.

Therein, by employing the PMP codes, the spectral decoder of the receiver can filter out most of the spectral components from unmatched transmitters. However, since the cross-correlation of the PMP codes is not zero, a few spectral components from unmatched transmitters can still pass through the spectral decoder. Hence, in order to eliminate these interferences, a pair of Mach–Zehnder interferometers and a balanced detector are employed in our proposed system in the light of [11].

Therein, the two arms of each Mach–Zehnder interferometer have different delay paths and hence will make optical signals passing through these two arms have different time delays. The difference of the time delays caused by the two arms is named differential path delay hereinafter.

It should be emphasized that the Mach–Zehnder interferometers in a matched pair of transmitter and receiver should have the same differential path delay $\tau$ that significantly exceeds $L\tau_c$ [12], where $L$ is the code length of PMP codes and $\tau_c$ is the source coherence time that can be defined as [10]

$$\tau_c = \frac{\int_0^\infty S^2(f)\,df}{\left[\int_0^\infty S(f)\,df\right]^2} \tag{7}$$

where $S(f)$ is the single sideband power spectral density of the source and $\int_0^\infty s(f)df$ is the output power of the source.

Moreover, different pairs of transmitters and receivers must have different differential path delays. The difference of these differential path delays must be at least 2–3 times of $L\tau_c$. In this way, the optical intensity noise due to the spectral components transmitted from unmatched transmitters can be completely eliminated.

Since the cross-correlation value between PMP code sequences in the same group is zero, the spectral components from other transmitters using the code sequences in the same group can be completely filtered out by the spectral decoder. Therefore, the transmitter and receiver pairs using same group code sequences won't interfere with each other even though the differential path delays of their Mach–Zehnder interferometer pairs are the same. Hence, the restriction on the differential path delays mentioned above can be relaxed, i.e., the transmitter and receiver pairs with same group code sequences can use Mach–Zehnder interferometer pairs with identical differential path delay.

## IV. Performance Analysis

To analyze system performance, we consider the intensity noise, shot noise and thermal noise. Gaussian approximation is employed to calculate the bit error rate (BER). In this paper, in order to suppress the effect of the thermal noise, we use APDs as the photodetectors. Hence, the variance of photocurrent noise resulted from detecting a thermal light (emitted by a broadband light source) can be expressed as [10]

$$\langle i^2\rangle = G^2P_{\rm in}^2R^2B\tau_c + 2eG^2F_eP_{\rm in}RB + 4K_bT_nB/R_L \tag{8}$$

where $G$ and $F_e$ are average gain and excess noise factor of an APD, $e$ is the electron's charge, $B$ is the noise-equivalent electrical bandwidth of the receiver, $\tau_c$ is coherence time of the light source, $K_b$ is Boltzmann's constant, $T_n$ is the absolute receiver noise temperature, $R_L$ is receiver load resistance, $P_{\rm in}$ refers to the optical power incident on the APD, and $R$ is the responsivity of the APD.

Therein, $R$ is given by $R = \eta e/hf_c$, where $\eta$ is the quantum efficiency of the APD, $h$ is the Planck's constant and $f_c$ is center operating frequency, and $P_{\rm in} = \int_0^\infty S(f)\,df$.

The items at right-hand side of (8) are results of the PIIN, shot noise and thermal noise, respectively. Therein, $F_e$ can be written as

$$F_e = k_eG + (1-k_e)(2-G^{-1}) \tag{9}$$

where $k_e$ is effective ionization ratio of the APD.

For analyzing the performance, the proposed system is modeled as illustrated in Fig. 2 by employing the method disclosed in [13], in which $h_{{\rm tr},a,i}(t), h_{{\rm tr},b,i}(t)$, $h_{{\rm re},a,i}(t)$, and $h_{{\rm re},b,i}(t)$ are the impulse responses of the arms of the Mach–Zehnder interferometers in the $i$th transmitter and receiver; $h_{{\rm tr,pmp},i}(t)$ and $h_{{\rm re,pmp},i}(t)$ are the impulse responses of the $i$th spectral encoder and decoder, respectively; $m_i(t)$ is the $i$th input data which can be "1" or "$-1$".

Furthermore, in order to simplify analysis, we make the following assumptions. First, the broadband light source is ideally unpolarized and has flat spectrum over $[f_c-\Delta f/2, f_c+\Delta f/2]$, where $f_c$ is the center frequency and $\Delta f$ is the bandwidth of the source (thus, $\tau_c = (\Delta f)^{-1}$). Secondly, the output powers of all broadband light sources are equal. Thirdly, the broadband light sources are mutually independent.

Based on these assumptions, the output of the $i$th transmitter can be expressed as

$$Z_i(t) = x_i(t) * \left[\frac{1}{2}h_{{\rm tr},a,i}(t) + \frac{1}{2}h_{{\rm tr},b,i}(t)m_i(t)e^{-j\pi}\right] * h_{{\rm tr,pmp},i}(t). \tag{10}$$

Hence, if there are $K$ users transmitting in the system simultaneously, the received optical signal of the $i$th receiver can be expressed as

$$R_i(t) = \frac{1}{\sqrt{N}} \sum_{j=1}^{K} x_j(t) * \left[ \frac{1}{2} h_{\mathrm{tr},a,j}(t) + \frac{1}{2} h_{\mathrm{tr},b,j}(t) m_j(t) e^{-j\pi} \right] * h_{\mathrm{tr,pmp},j}(t). \quad (11)$$

Although the input data of the transmitters can be "1" or "−1" arbitrarily, the induced noise effects are the same. For simplicity, we take all of the input data to be "1". Since the broadband light sources are mutually independent, the power spectral density (PSD) of the received signal can be written as

$$S_{R_i R_i^*}(f) = \frac{1}{4N} \sum_{j=1}^{K} S_{x_j x_j^*}(f) |H_{\mathrm{tr},a,j}(f) - H_{\mathrm{tr},b,j}(f)|^2 |H_{\mathrm{tr,pmp},j}(f)|^2 \quad (12)$$

where $S_{x_j x_j^*}(f)$ is the power spectral density of the output beam due to the $j$th broadband light source; $H_{\mathrm{tr},a,j}(f)$ and $H_{\mathrm{tr},b,j}(f)$ are the transfer functions of the arms of the Mach–Zehnder interferometers in the $j$th transmitter; $H_{\mathrm{tr,pmp},j}(f)$ is the transfer function of the $j$th spectral encoder.

After passing the spectral decoder and the Mach–Zehnder interferometer of the $i$th receiver, the optical signals incident on the APDs of the $i$th balanced detector can be respectively expressed as

$$W_a(t) = R_i(t) * h_{\mathrm{re,pmp},i}(t) * \left[ \frac{1}{2} h_{\mathrm{re},a,i}(t) + \frac{1}{2} h_{\mathrm{re},b,i}(t) e^{-j\pi} \right], \quad (13)$$

and

$$W_b(t) = R_i(t) * h_{\mathrm{re,pmp},i}(t) * \left[ \frac{1}{2} h_{\mathrm{re},a,i}(t) e^{-j\pi/2} + \frac{1}{2} h_{\mathrm{re},b,i}(t) e^{-j\pi/2} \right] \quad (14)$$

where $W_a$ and $W_b$ represent the optical signals respectively incident on the APDs of the $i$th balanced detector.

Their power spectral densities can be expressed as

$$\begin{aligned} S_{W_a W_a^*}(f) &= \frac{1}{4} S_{R_i R_i^*}(f) |H_{\mathrm{re,pmp},i}(f)|^2 \times |H_{\mathrm{re},a,i}(f) - H_{\mathrm{re},b,i}(f)|^2 \\ &= \frac{1}{16N} \sum_{j=1}^{K} S_{x_j x_j^*}(f) |H_{\mathrm{tr},a,j}(f) - H_{\mathrm{tr},b,j}(f)|^2 |H_{\mathrm{tr,pmp},j}(f)|^2 \\ &\quad \cdot |H_{\mathrm{re,pmp},i}(f)|^2 |H_{\mathrm{re},a,i}(f) - H_{\mathrm{re},b,i}(f)|^2 \end{aligned} \quad (15)$$

and

$$\begin{aligned} S_{W_b W_b^*}(f) &= \frac{1}{4} S_{R_i R_i^*}(f) |H_{\mathrm{re,pmp},i}(f)|^2 \times |H_{\mathrm{re},a,i}(f) + H_{\mathrm{re},b,i}(f)|^2 \\ &= \frac{1}{16N} \sum_{j=1}^{K} S_{x_j x_j^*}(f) |H_{\mathrm{tr},a,j}(f) - H_{\mathrm{tr},b,j}(f)|^2 |H_{\mathrm{tr,pmp},j}(f)|^2 \\ &\quad \cdot |H_{\mathrm{re,pmp},i}(f)|^2 |H_{\mathrm{re},a,i}(f) + H_{\mathrm{re},b,i}(f)|^2, \end{aligned} \quad (16)$$

where $H_{\mathrm{re},a,j}(f)$ and $H_{\mathrm{re},b,j}(f)$ are the transfer functions of the arms of the Mach–Zehnder interferometer in the $j$th receiver; $H_{\mathrm{re,pmp},j}(f)$ is the transfer function of the $j$th spectral decoder. Consequently, the net photocurrent $I$ in the $i$th balanced detector can be written as

$$\begin{aligned} I &= I_a - I_b \\ &= GR \left[ \int_0^\infty S_{W_a W_a^*}(f)\, df - \int_0^\infty S_{W_b W_b^*}(f)\, df \right] \end{aligned} \quad (17)$$

where $I_a$ and $I_b$ are the photocurrents outputted from the APDs, respectively.

Now, in order to further compute the photocurrent $I$, we associate the transfer functions of the decoders and encoders with the PMP codes and define a new function as following:

$$\begin{aligned} S_{mn}(f) &= S_{x_m x_m^*}(f) |H_{\mathrm{tr,pmp},m}(f)|^2 |H_{\mathrm{re,pmp},n}(f)|^2 \\ &= \frac{P_s}{\Delta f} \sum_{g=1}^{L} C_m(g) C_n(g) F(g,f), \end{aligned} \quad (18)$$

where $m, n \in (1, 2 \ldots K)$, $P_s$ is the output power of the broadband light source and $F(\mathrm{g})$ is the $g$th spectral element of the encoder or decoder and can be expressed as

$$F(g,f) = \left\{ u\left[ f - f_c - \frac{\Delta f}{2L}(-L + 2g - 2) \right] - u\left[ f - f_c - \frac{\Delta f}{2L}(-L + 2g) \right] \right\} \quad (19)$$

where $u(f)$ is the unit step function defined as

$$u(f) = \begin{cases} 1, & f \geq 0 \\ 0, & f < 0. \end{cases} \quad (20)$$

In order to completely eliminate the MUI, the transfer functions of the arms of the interferometers in the transmitters and receivers should be orthogonal to each other, except for the transfer functions belonging to matched transmitters and receivers, which should be either equal or complex conjugates. These conditions can be expressed mathematically as [13]

$$H_{\mathrm{tr},a,m} \perp H_{\mathrm{tr},b,n} \quad \forall m, n \quad (21)$$

$$H_{\mathrm{tr},a,m} \perp H_{\mathrm{tr},a,n} \quad \forall m \neq n \quad (22)$$

$$H_{\mathrm{tr},b,m} \perp H_{\mathrm{tr},b,n} \quad \forall m \neq n \quad (23)$$

$$H_{\mathrm{tr},a,m} \perp H_{\mathrm{re},a,n} \quad \forall m \neq n \quad (24)$$

$$H_{\mathrm{tr},b,m} \perp H_{\mathrm{re},b,n} \quad \forall m \neq n \quad (25)$$

$$(H_{\mathrm{tr},a,m} = H_{\mathrm{re},a,m} \cap H_{\mathrm{tr},b,m} = H_{\mathrm{re},b,m}\ \forall m) \bigcup (H_{\mathrm{tr},a,m}^* = H_{\mathrm{re},a,m} \cap H_{\mathrm{tr},b,m}^* = H_{\mathrm{re},b,m}\ \forall m). \quad (26)$$

Substituting (15), (16), and (18) into (17), we have the photocurrent $I$ as:

$$I = \frac{GR}{8N} \int_0^\infty \sum_{j=1}^{K} S_{ji}(f) |H_{\mathrm{tr},a,j}(f) - H_{\mathrm{tr},b,j}(f)|^2 \cdot [-H_{\mathrm{re},a,i}(f) H_{\mathrm{re},b,i}^*(f) - H_{\mathrm{re},a,i}^*(f) H_{\mathrm{re},b,i}(f)]\, df. \quad (27)$$

Using (24) and (25), we can show that the interferences from unmatched transmitters are all filtered out and the photocurrent reduces to

$$I = \frac{GR}{8N}\int_0^\infty S_{ii}(f)|H_{\mathrm{tr},a,i}(f) - H_{\mathrm{tr},b,i}(f)|^2 \cdot [-H_{\mathrm{re},a,i}(f)H^*_{\mathrm{re},b,i}(f) - H^*_{\mathrm{re},a,i}(f)H_{\mathrm{re},b,i}(f)]\,df \quad (28)$$

$$= \frac{GR}{8N}\int_0^\infty S_{ii}(f)[|H_{\mathrm{tr},a,i}(f)|^2 - H_{\mathrm{tr},a,i}(f)H^*_{\mathrm{tr},b,i}(f) - H^*_{\mathrm{tr},a,i}(f)H_{\mathrm{tr},b,i}(f) + |H_{\mathrm{tr},b,i}(f)|^2] \cdot [-H_{\mathrm{re},a,i}(f)H^*_{\mathrm{re},b,i}(f) - H^*_{\mathrm{re},a,i}(f)H_{\mathrm{re},b,i}(f)]\,df. \quad (29)$$

Using (21) and (26), we have

$$I = \frac{GR}{8N}\int_0^\infty S_{ii}(f)[H_{\mathrm{tr},a,i}(f)H^*_{\mathrm{tr},b,i}(f)H^*_{\mathrm{re},a,i}(f)H_{\mathrm{re},b,i}(f) + H^*_{\mathrm{tr},a,i}(f)H_{\mathrm{tr},b,i}(f)H_{\mathrm{re},a,i}(f)H^*_{\mathrm{re},b,i}(f)]\,df \quad (30)$$

$$= \frac{GR}{4N}\int_0^\infty S_{ii}(f)|H_{\mathrm{tr},a,i}(f)|^2|H_{\mathrm{tr},b,i}(f)|^2\,df. \quad (31)$$

Then, substituting (18) into (31), we can rewrite the photocurrent as

$$I = \frac{GR}{4N}\int_0^\infty \left[\frac{P_s}{\Delta f}\sum_{g=1}^{L} C_i(g)C_i(g)F(g,f)\right] \times |H_{\mathrm{tr},a,i}(f)|^2|H_{\mathrm{tr},b,i}(f)|^2\,df \quad (32)$$

$$= \frac{GP_sR}{4N\Delta f}\int_0^\infty |H_{\mathrm{tr},a,i}(f)|^2|H_{\mathrm{tr},b,i}(f)|^2 \times \sum_{g=1}^{L} C_i(g)F(g,f)\,df \quad (33)$$

$$= \frac{GP_sR}{4N\Delta f}\left[\frac{(p-1)}{M}\cdot\frac{\Delta f}{L}\right]. \quad (34)$$

Finally, with $L = p^2$, we obtain the photocurrent as

$$I = \frac{GP_sR(p-1)}{4NMp^2}. \quad (35)$$

According to (7) and (8), the PIIN can be rewritten as

$$\langle i^2_{\mathrm{PIIN}}\rangle = G^2P^2_{\mathrm{in}}R^2B\tau_c, \quad (36)$$

$$= G^2R^2B\int_0^\infty S^2(f)\,df. \quad (37)$$

Accordingly, the PIIN at the receiving end can be expressed as

$$\langle i^2_{\mathrm{PIIN}}\rangle = BG^2R^2\int_0^\infty \left[S_{W_bW_b^*}(f) - S_{W_aW_a^*}(f)\right]^2 df \quad (38)$$

$$= \frac{BG^2R^2}{64N^2}\int_0^\infty [H_{\mathrm{re},a,i}(f)H^*_{\mathrm{re},b,i}(f) + H^*_{\mathrm{re},a,i}(f)H_{\mathrm{re},b,i}(f)]^2 \cdot \left[\sum_{j=1}^{K}S_{ji}(f)|H_{\mathrm{tr},a,j}(f) - H_{\mathrm{tr},b,j}(f)|^2\right]^2 df \quad (39)$$

$$= \frac{BG^2R^2P_s^2}{64N^2\Delta f^2}\int_0^\infty [H_{\mathrm{re},a,i}(f)H^*_{\mathrm{re},b,i}(f) + H^*_{\mathrm{re},a,i}(f)H_{\mathrm{re},b,i}(f)]^2 \cdot \left[\sum_{j=1}^{K}\sum_{h=1}^{K}|H_{\mathrm{tr},a,j}(f) - H_{\mathrm{tr},b,j}(f)|^2 \times |H_{\mathrm{tr},a,h}(f) - H_{\mathrm{tr},b,h}(f)|^2 \cdot \sum_{g=1}^{L}C_i(g)C_j(g)C_h(g)F(g,f)\right] df. \quad (40)$$

In order to simplify notations, we will express (40) as

$$\langle i^2_{\mathrm{PIIN}}\rangle = N_1 + N_2 + N_3 + N_4, \quad (41)$$

where $N_1$, $N_2$, $N_3$, and $N_4$ represent the noises for $j = h = i$, $j = i \neq h \cup j \neq i = h$, $j = h \neq i$, and $j \neq h \neq i$, respectively.

For $j = h = i$, the PIIN noise can be expressed as

$$N_1 = \frac{BG^2R^2P_s^2}{64N^2\Delta f^2} \times \int_0^\infty \left[H_{\mathrm{re},a,i}(f)H^*_{\mathrm{re},b,i}(f) + H^*_{\mathrm{re},a,i}(f)H_{\mathrm{re},b,i}(f)\right]^2 \cdot |H_{\mathrm{tr},a,i}(f) - H_{\mathrm{tr},b,i}(f)|^4\sum_{g=1}^{L}C_i(g)F(g,f)\,df \quad (42)$$

$$= \frac{BG^2R^2P_s^2}{64N^2\Delta f^2} \cdot \int_0^\infty \{[H_{\mathrm{re},a,i}(f)H^*_{\mathrm{re},b,i}(f)]^2 + [H^*_{\mathrm{re},a,i}(f)H_{\mathrm{re},b,i}(f)]^2 + 2|H_{\mathrm{re},a,i}(f)|^2|H_{\mathrm{re},b,i}(f)|^2\} \cdot \{|H_{\mathrm{tr},a,i}(f)|^4 + |H_{\mathrm{tr},b,i}(f)|^4 + 4|H_{\mathrm{tr},a,i}(f)|^2|H_{\mathrm{tr},b,i}(f)|^2 + [H_{\mathrm{tr},a,i}(f)H^*_{\mathrm{tr},b,i}(f)]^2 + [H^*_{\mathrm{tr},a,i}(f)H_{\mathrm{tr},b,i}(f)]^2 - 2|H_{\mathrm{tr},a,i}(f)|^2[H_{\mathrm{tr},a,i}(f)H^*_{\mathrm{tr},b,i}(f) + H^*_{\mathrm{tr},a,i}(f)H_{\mathrm{tr},b,i}(f)] - 2|H_{\mathrm{tr},b,i}(f)|^2[H_{\mathrm{tr},a,i}(f)H^*_{\mathrm{tr},b,i}(f) + H^*_{\mathrm{tr},a,i}(f)H_{\mathrm{tr},b,i}(f)]\} \cdot \sum_{g=1}^{L}C_i(g)F(g,f)\,df. \quad (43)$$

Using (21) and (26), we have

$$N_1 = \frac{BG^2R^2P_s^2}{64N^2\Delta f^2}\int_0^\infty \{2|H_{\mathrm{tr},a,i}(f)|^6|H_{\mathrm{tr},b,i}(f)|^2 + 2|H_{\mathrm{tr},a,i}(f)|^2|H_{\mathrm{tr},b,i}(f)|^6 + 10|H_{\mathrm{tr},a,i}(f)|^4|H_{\mathrm{tr},b,i}(f)|^4\} \cdot \sum_{g=1}^{L}C_i(g)F(g,f)\,df \quad (44)$$

$$= \frac{BG^2R^2P_s^2}{64N^2\Delta f^2}\cdot\left[\frac{14(p-1)\Delta f}{ML}\right]. \quad (45)$$

For $j = i \neq h \cup j \neq i = h$, since the situation with $j = i \neq h$ is the same as that with $j \neq i = h$, we need only to evaluate one

of them and then double the result. Thus, the PIIN noise can be expressed as

$$\begin{aligned}N_2 = 2\times\frac{BG^2R^2P_s^2}{64N^2\Delta f^2}\int_0^\infty &[H_{\mathrm{re},a,i}(f)H^*_{\mathrm{re},b,i}(f)\\ &+H^*_{\mathrm{re},a,i}(f)H_{\mathrm{re},b,i}(f)]^2\\ &\cdot\left[\sum_{\substack{h=1\\h\neq i}}^{K}|H_{\mathrm{tr},a,i}(f)-H_{\mathrm{tr},b,i}(f)|^2\right.\\ &\times|H_{\mathrm{tr},a,h}(f)-H_{\mathrm{tr},b,h}(f)|^2\\ &\left.\cdot\sum_{g=1}^{L}C_i(g)C_h(g)F(g,f)\right]df \qquad (46)\\ =2\times\frac{BG^2R^2P_s^2}{64N^2\Delta f^2}\sum_{\substack{h=1\\h\neq i}}^{K}\int_0^\infty &\{[H_{\mathrm{re},a,i}(f)H^*_{\mathrm{re},b,i}(f)]^2\\ &+[H^*_{\mathrm{re},a,i}(f)H_{\mathrm{re},b,i}(f)]^2\\ &+2|H_{\mathrm{re},a,i}(f)|^2|H_{\mathrm{re},b,i}(f)|^2\}\\ &\cdot\{[|H_{\mathrm{tr},a,i}(f)|^2+|H_{\mathrm{tr},b,i}(f)|^2-H_{\mathrm{tr},a,i}(f)H^*_{\mathrm{tr},b,i}(f)\\ &-H^*_{\mathrm{tr},a,i}(f)H_{\mathrm{tr},b,i}(f)]\cdot[|H_{\mathrm{tr},a,h}(f)|^2+|H_{\mathrm{tr},b,h}(f)|^2\\ &-H_{\mathrm{tr},a,h}(f)H^*_{\mathrm{tr},b,h}(f)-H^*_{\mathrm{tr},a,h}(f)H_{\mathrm{tr},b,h}(f)]\}\\ &\cdot\sum_{g=1}^{L}C_i(g)C_h(g)F(g,f)\,df. \qquad (47)\end{aligned}$$

For $N_2$, we have

$$\begin{aligned}N_2 = 2\times\frac{BG^2R^2P_s^2}{64N^2\Delta f^2}&\times\sum_{\substack{h=1\\h\neq i}}^{K}\int_0^\infty 2|H_{\mathrm{re},a,i}(f)|^2|H_{\mathrm{re},b,i}(f)|^2\\ &\times\{[|H_{\mathrm{tr},a,i}(f)|^2+|H_{\mathrm{tr},b,i}(f)|^2]\\ &\cdot[|H_{\mathrm{tr},a,h}(f)|^2+|H_{\mathrm{tr},b,h}(f)|^2]\}\\ &\cdot\sum_{g=1}^{L}C_i(g)C_h(g)F(g,f)\,df. \qquad (48)\end{aligned}$$

Furthermore, since the code weight of the PMP code is $(p-1)/M$, each code sequence will be beaten by other $(p-1)(p-2)/M$ code sequences. Because the code size is $Mp^2$, the probability that a code sequence being beaten by another code sequence is

$$P_{\mathrm{hit}}=\frac{(p-1)(p-2)}{M(Mp^2-1)}. \qquad (49)$$

Therefore, $N_2$ can be further expressed as

$$\begin{aligned}N_2 &= 2\times\frac{BG^2R^2P_s^2}{64N^2\Delta f^2}\cdot\left[\frac{8(K-1)P_{\mathrm{hit}}\Delta f}{L}\right] \qquad (50)\\ &=\frac{\mathrm{BR}^2P_s^2}{64N^2\Delta f^2}\cdot\left[\frac{16(K-1)(p-1)(p-2)\Delta f}{ML(Mp^2-1)}\right]. \qquad (51)\end{aligned}$$

Likewise, for $j=h\neq i$, the PIIN noise can be expressed as

$$\begin{aligned}N_3 = \frac{BG^2R^2P_s^2}{64N^2\Delta f^2}\int_0^\infty &[H_{\mathrm{re},a,i}(f)H^*_{\mathrm{re},b,i}(f)\\ &+H^*_{\mathrm{re},a,i}(f)H_{\mathrm{re},b,i}(f)]^2\\ &\cdot\left[\sum_{\substack{h=1\\h\neq i}}^{K}(|H_{\mathrm{tr},a,h}(f)-H_{\mathrm{tr},b,h}(f)|^2)^2\right.\\ &\left.\times\sum_{g=1}^{L}C_i(g)C_h(g)F(g,f)\right]df \qquad (52)\\ =\frac{BG^2R^2P_s^2}{64N^2\Delta f^2}\cdot\sum_{\substack{h=1\\h\neq i}}^{K}\int_0^\infty &\{[H_{\mathrm{re},a,i}(f)H^*_{\mathrm{re},b,i}(f)]^2\\ &+[H^*_{\mathrm{re},a,i}(f)H_{\mathrm{re},b,i}(f)]^2+2|H_{\mathrm{re},a,i}(f)|^2|H_{\mathrm{re},b,i}(f)|^2\}\\ &\cdot\{|H_{\mathrm{tr},a,h}(f)|^4+|H_{\mathrm{tr},b,h}(f)|^4\\ &+4|H_{\mathrm{tr},a,h}(f)|^2|H_{\mathrm{tr},b,h}(f)|^2\\ &+[H_{\mathrm{tr},a,h}(f)H^*_{\mathrm{tr},b,h}(f)]^2+[H^*_{\mathrm{tr},a,h}(f)H_{\mathrm{tr},b,h}(f)]^2\\ &-2|H_{\mathrm{tr},a,h}(f)|^2[H_{\mathrm{tr},a,h}(f)H^*_{\mathrm{tr},b,h}(f)\\ &+H^*_{\mathrm{tr},a,h}(f)H_{\mathrm{tr},b,h}(f)]\\ &-2|H_{\mathrm{tr},b,h}(f)|^2[H_{\mathrm{tr},a,h}(f)H^*_{\mathrm{tr},b,h}(f)\\ &+H^*_{\mathrm{tr},a,h}(f)H_{\mathrm{tr},b,h}(f)]\}\\ &\cdot\sum_{g=1}^{L}C_i(g)F(g,f)\,df. \qquad (53)\end{aligned}$$

For $N_3$, we have

$$\begin{aligned}N_3 = \frac{BG^2R^2P_s^2}{64N^2\Delta f^2}\cdot\sum_{\substack{h=1\\h\neq i}}^{K}\int_0^\infty &2|H_{\mathrm{re},a,i}(f)|^2|H_{\mathrm{re},b,i}(f)|^2\\ &\times\{|H_{\mathrm{tr},a,h}(f)|^4+|H_{\mathrm{tr},b,h}(f)|^4\\ &+4|H_{\mathrm{tr},a,h}(f)|^2|H_{\mathrm{tr},b,h}(f)|^2\}\\ &\cdot\sum_{g=1}^{L}C_i(g)F(g,f)\,df \qquad (54)\\ =\frac{BG^2R^2P_s^2}{64N^2\Delta f^2}&\cdot\left[\frac{12(K-1)P_{\mathrm{hit}}\Delta f}{L}\right] \qquad (55)\\ =\frac{BG^2R^2P_s^2}{64N^2\Delta f^2}&\cdot\left[\frac{12(K-1)(p-1)(p-2)\Delta f}{ML(Mp^2-1)}\right]. \qquad (56)\end{aligned}$$

Finally, for $j\neq h\neq i$, the PIIN noise can be expressed as

$$\begin{aligned}N_4 = \frac{BG^2R^2P_s^2}{64N^2\Delta f^2}\int_0^\infty &[H_{\mathrm{re},a,i}(f)H^*_{\mathrm{re},b,i}(f)\\ &+H^*_{\mathrm{re},a,i}(f)H_{\mathrm{re},b,i}(f)]^2\\ &\cdot\left[\sum_{\substack{j=1\\j\neq i}}^{K}\sum_{\substack{h=1\\h\neq i,j}}^{K}|H_{\mathrm{tr},a,j}(f)-H_{\mathrm{tr},b,j}(f)|^2\right.\\ &\times|H_{\mathrm{tr},a,h}(f)-H_{\mathrm{tr},b,h}(f)|^2\\ &\left.\cdot\sum_{g=1}^{L}C_i(g)C_j(g)C_h(g)F(g,f)\right]df \qquad (57)\end{aligned}$$

$$= \frac{BG^2R^2P_s^2}{64N^2\Delta f^2}\sum_{\substack{j=1\\ j\neq i}}^{K}\sum_{\substack{h=1\\ h\neq i,j}}^{K}\int_0^\infty \{[H_{\mathrm{re},a,i}(f)H^*_{\mathrm{re},b,i}(f)]^2 + [H^*_{\mathrm{re},a,i}(f)H_{\mathrm{re},b,i}(f)]^2 + 2|H_{\mathrm{re},a,i}(f)|^2|H_{\mathrm{re},b,i}(f)|^2\} \cdot \{[|H_{\mathrm{tr},a,j}(f)|^2 + |H_{\mathrm{tr},b,j}(f)|^2 - H_{\mathrm{tr},a,j}(f)H^*_{\mathrm{tr},b,j}(f) - H^*_{\mathrm{tr},a,j}(f)H_{\mathrm{tr},b,j}(f)] \cdot [|H_{\mathrm{tr},a,h}(f)|^2 + |H_{\mathrm{tr},b,h}(f)|^2 - H_{\mathrm{tr},a,h}(f)H^*_{\mathrm{tr},b,h}(f) - H^*_{\mathrm{tr},a,h}(f)H_{\mathrm{tr},b,h}(f)]\} \cdot \sum_{g=1}^{L} C_i(g)C_h(g)F(g,f)\,df. \quad (58)$$

Using (21)–(23) and (26), we have

$$N_4 = \frac{BG^2R^2P_s^2}{64N^2\Delta f^2}\sum_{\substack{j=1\\ j\neq i}}^{K}\sum_{\substack{h=1\\ h\neq i,j}}^{K}\int_0^\infty 2|H_{\mathrm{re},a,i}(f)|^2|H_{\mathrm{re},b,i}(f)|^2 \times [|H_{\mathrm{tr},a,j}(f)|^2 + |H_{\mathrm{tr},b,j}(f)|^2] \cdot [|H_{\mathrm{tr},a,h}(f)|^2 + |H_{\mathrm{tr},b,h}(f)|^2] \cdot \sum_{g=1}^{L} C_i(g)C_h(g)F(g,f)df. \quad (59)$$

Since the probability for code sequences $C_j(g)$ and $C_h(g)$ to beat the same spectral element of is

$$P'_{\mathrm{hit}} = P_{\mathrm{hit}}\frac{(p-3)}{(Mp^2-2)} = \frac{(p-1)(p-2)(p-3)}{M(Mp^2-1)(Mp^2-2)}. \quad (60)$$

$N_4$ can be further expressed as

$$N_4 = \frac{BG^2R^2P_s^2}{64N^2\Delta f^2}\cdot\left[\frac{8(K-1)(K-2)P'_{\mathrm{hit}}\Delta f}{L}\right] \quad (61)$$

$$= \frac{BG^2R^2P_s^2}{64N^2\Delta f^2} \cdot \left[\frac{8(K-1)(K-2)(p-1)(p-2)(p-3)\Delta f}{ML(Mp^2-1)(Mp^2-2)}\right]. \quad (62)$$

Therefore, the total PIIN is given as

$$\langle i^2_{\mathrm{PIIN}}\rangle = \frac{BG^2R^2P_s^2}{64N^2\Delta f^2}\left\{\left[\frac{14(p-1)\Delta f}{ML}\right] + \left[\frac{16(K-1)(p-1)(p-2)\Delta f}{ML(Mp^2-1)}\right] + \left[\frac{12(K-1)(p-1)(p-2)\Delta f}{ML(Mp^2-1)}\right] + \left[\frac{8(K-1)(K-2)(p-1)(p-2)(p-3)\Delta f}{ML(Mp^2-1)(Mp^2-2)}\right]\right\} \quad (63)$$

$$= \frac{BG^2R^2P_s^2(p-1)}{64N^2ML\Delta f}\left\{14 + \frac{4(K-1)(p-2)}{(Mp^2-1)} \times \left[7 + \frac{2(K-2)(p-3)}{(Mp^2-2)}\right]\right\}. \quad (64)$$

Furthermore, applying (8), we can express the shot noise in the receiver as

$$\langle i^2_{\mathrm{shot}}\rangle = 2eG^2F_eRB\left[\int_0^\infty S^*_{W_aW_a}(f)\,df + \int_0^\infty S^*_{W_bW_b}(f)\,df\right] \quad (65)$$

$$= \frac{eG^2F_eRB}{8N}\int_0^\infty \sum_{j=1}^{K} S_{x_jx_j^*}(f)|H_{\mathrm{tr},a,j}(f) - H_{\mathrm{tr},b,j}(f)|^2|H_{\mathrm{tr,pmp},j}(f)|^2 \cdot |H_{\mathrm{re,pmp},i}(f)|^2[|H_{\mathrm{re},a,i}(f) - H_{\mathrm{re},b,i}(f)|^2 + |H_{\mathrm{re},a,i}(f) + H_{\mathrm{re},b,i}(f)|^2]\,df \quad (66)$$

$$= \frac{eP_sG^2F_eRB(p-1)}{NMp^2}\left[1 + \frac{(K-1)(p-2)}{(Mp^2-1)}\right]. \quad (67)$$

The total noise power including PIIN, shot noise, and thermal noise can be expressed as

$$\langle i^2\rangle = \frac{BG^2R^2P_s^2(p-1)}{64N^2ML\Delta f}\left\{14 + \frac{4(K-1)(p-2)}{(Mp^2-1)} \times \left[7 + \frac{2(K-2)(p-3)}{(Mp^2-2)}\right]\right\} + \frac{eBG^2F_eP_sR(p-1)}{NMp^2}\left[1 + \frac{(K-1)(p-2)}{(Mp^2-1)}\right] + 4K_bT_nB/R_L. \quad (68)$$

Consequently, the signal-to-noise ratio (SNR) at a receiver in the proposed system with PMP codes can be obtained as shown in (69) shown at the bottom of the page. The bit error rate (BER) can then be estimated from SNR as [11]

$$\mathrm{BER} = Q(\sqrt{\mathrm{SNR}}) \quad (70)$$

where

$$Q(x) = \frac{1}{\sqrt{2\pi}}\int_x^\infty \exp\left(\frac{-z^2}{2}\right)dz. \quad (71)$$

## V. Numerical and Simulation Results

The system parameters used to obtain the numerical results are listed in Table III. We assume the quantum efficiency, average gain, excess noise factor and effective ionization ratio of

$$\mathrm{SNR} = \frac{I^2}{\langle i^2\rangle} = \frac{\frac{G^2P_s^2R^2(p-1)^2}{16N^2M^2p^4}}{\frac{BG^2R^2P_s^2(p-1)}{64N^2ML\Delta f}\left\{14 + \frac{4(K-1)(p-2)}{(Mp^2-1)}\left[7 + \frac{2(K-2)(p-3)}{(Mp^2-2)}\right]\right\} + \frac{eBG^2F_eP_sR(p-1)}{NMp^2}\left[1 + \frac{(K-1)(p-2)}{(Mp^2-1)}\right] + 4K_bT_nB/R_L}. \quad (69)$$

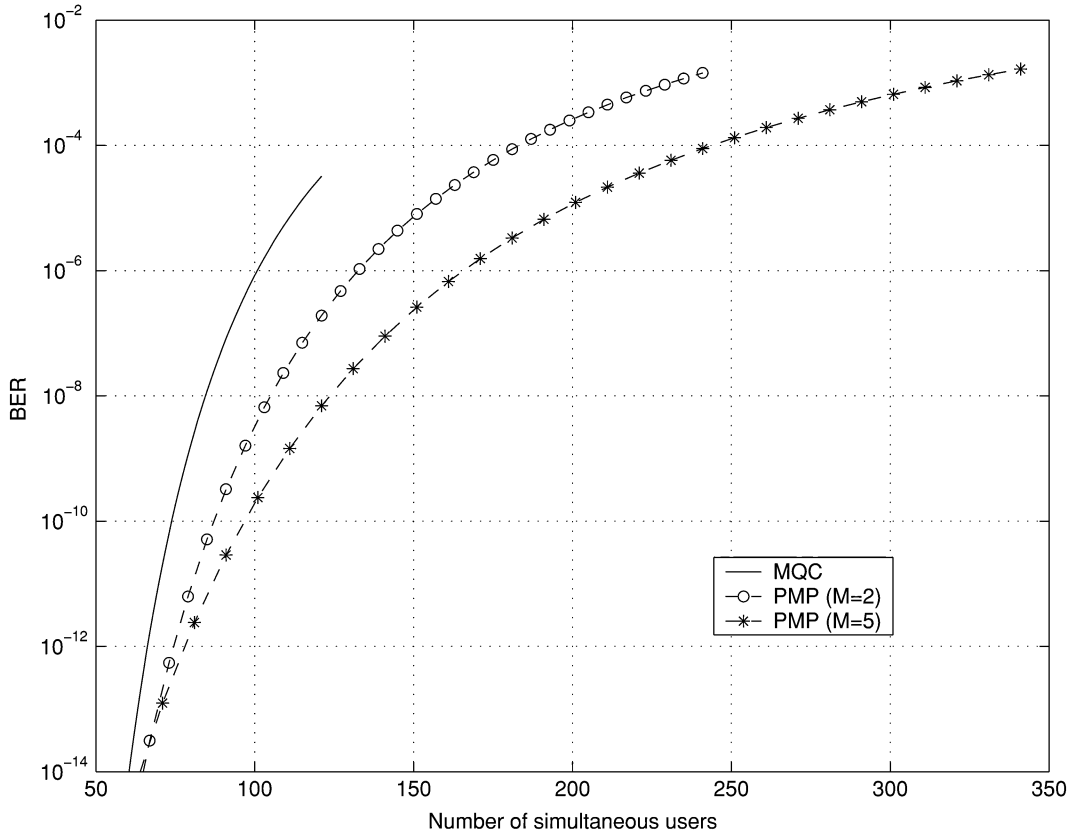


Fig. 3. The number of simultaneous users versus the BER for $p = 11$ at the effective source power equal to $-5$ dBm.

TABLE III
PARAMETERS USED IN THE NUMERICAL CALCULATION

| | |
|---|---|
| PD quantum efficiency | $\eta$=0.6 |
| Spectral width of broadband light source | $\Delta\lambda$=30nm (i.e. $\Delta f$=3.75THz) |
| Coherence time of broadband light source | $\tau_c \approx 0.267$ ps |
| Wavelength location | 1.55μm |
| Average gain of APD | $G$=40 |
| Effective ionization ratio of APD | $k_e$=0.5 |
| Excess noise factor of APD | $F_e \approx 21$ |
| Electrical bandwidth | $B$=80MHz |
| Data transmission rate | 155Mbps |
| Receiver noise temperature | $T_n$=300K |
| Receiver load resistor | $R_L$=1030Ω |

the APDs are $\eta = 0.6$, $G = 40$, $F_e \approx 21$, and $k_e = 0.5$, respectively. The receiver noise temperature and load resistance are $T_n = 300$ K and $R_L = 1030\,\Omega$. The spectrum of the broadband light source is centered at 1.55 $\mu$m with spectral width $\Delta\lambda = 30$ nm and coherence time is about $\tau_c \approx 0.267$ ps. The data transmission rate is 155 Mb/s and the electrical bandwidth of receivers is 80 MHz.

Figs. 3 and 4 show the maximum number of simultaneous users of our proposed system using PMP codes versus the BER for $p = 11$ and 13, with the effective source power fixed at $-5$ dBm (the effective source power is $\alpha P_s$, in which $\alpha$ is the loss due to transmission and star coupler and equal to $1/N$ when transmission loss is ignored). For comparison, the maximum number of simultaneous users for a system using MQC codes is also shown [10].

In Fig. 3, we have $p = 11$ and $M = 2$ or 5, the code length is 121. Thus, the code size can be 242 or 605. Since each code sequence can be assigned to a different subscriber, the maximum number of the subscribers in our proposed system can reach 242 or 605. For comparison, we also consider the MQC code with $p = 11$, whose code length and code size are 132 and 121, respectively. This figure shows that the proposed system has better performance than the system using MQC codes for both $M = 2$ and $M = 5$.

In Fig. 4, $p = 13$ and $M$ can be 2, 3, or 4. The code length is 169. Hence, the code size can be 338, 507 or 676, respectively. The MQC code has $p = 13$ and its code length and code size are 182 and 169, respectively. Similarly, Fig. 4 shows that our proposed system has better performance than the system using MQC codes.

Moreover, the proposed system architecture can also be applied to an Ethernet passive optical network (EPON). Assuming the maximum subscriber number of EPON to be 32, the PMP code with $p = 5$ and $M = 2$ is used to obtain the numerical results shown in Figs. 5, where the code length is 25 and the code size is 50. The electrical bandwidth and data transmission rate shown in Table III are changed to 320 MHz and 622 Mb/s, respectively.

Fig. 5 shows the number of simultaneous users of the proposed system versus the BER with the effective source power fixed at $-5$ dBm. For comparison, the numbers of simultaneous users for a system using the MQC code with $p = 5$, whose code length is 30 and code size is 25, are also shown.

As the received optical power is fixed at $-5$ dBm, the proposed system can accommodate about 35 simultaneous users and the system using MQC code can accommodate 25 simultaneous users (limited by its code size) at $\mathrm{BER} = 10^{-9}$. It means

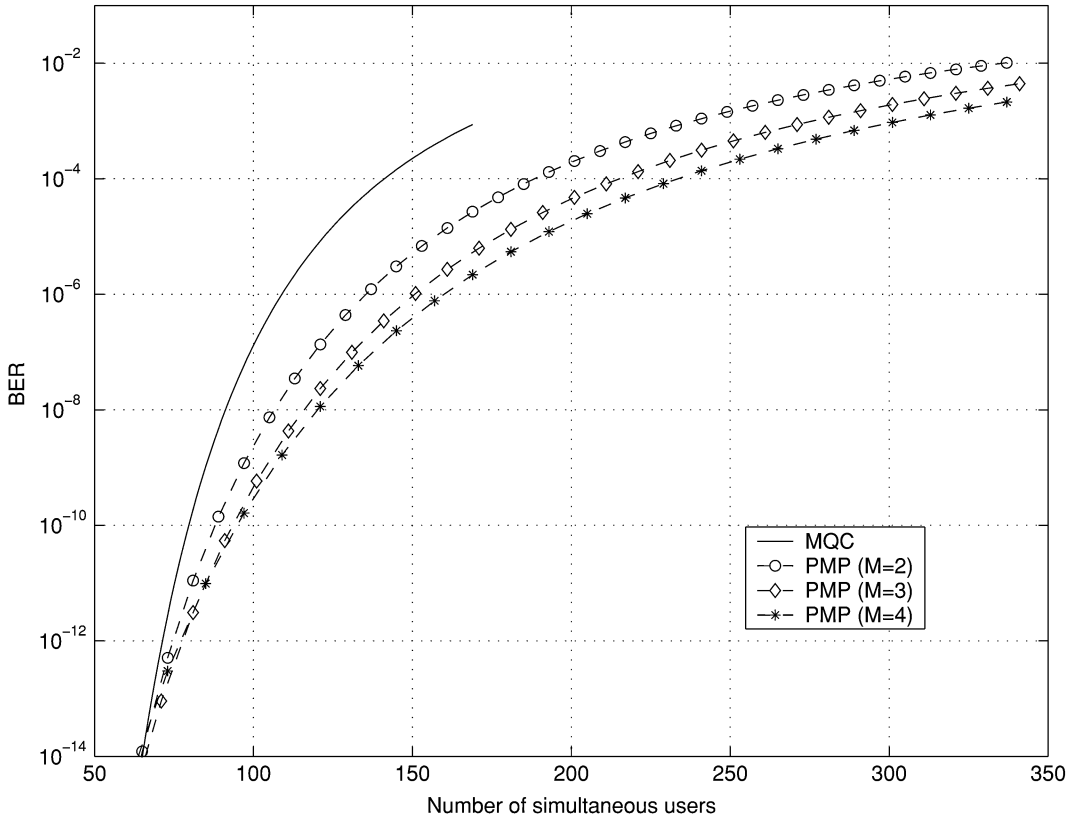


Fig. 4. The number of simultaneous users versus the BER for $p = 13$ at the effective source power equal to $-5$ dBm.

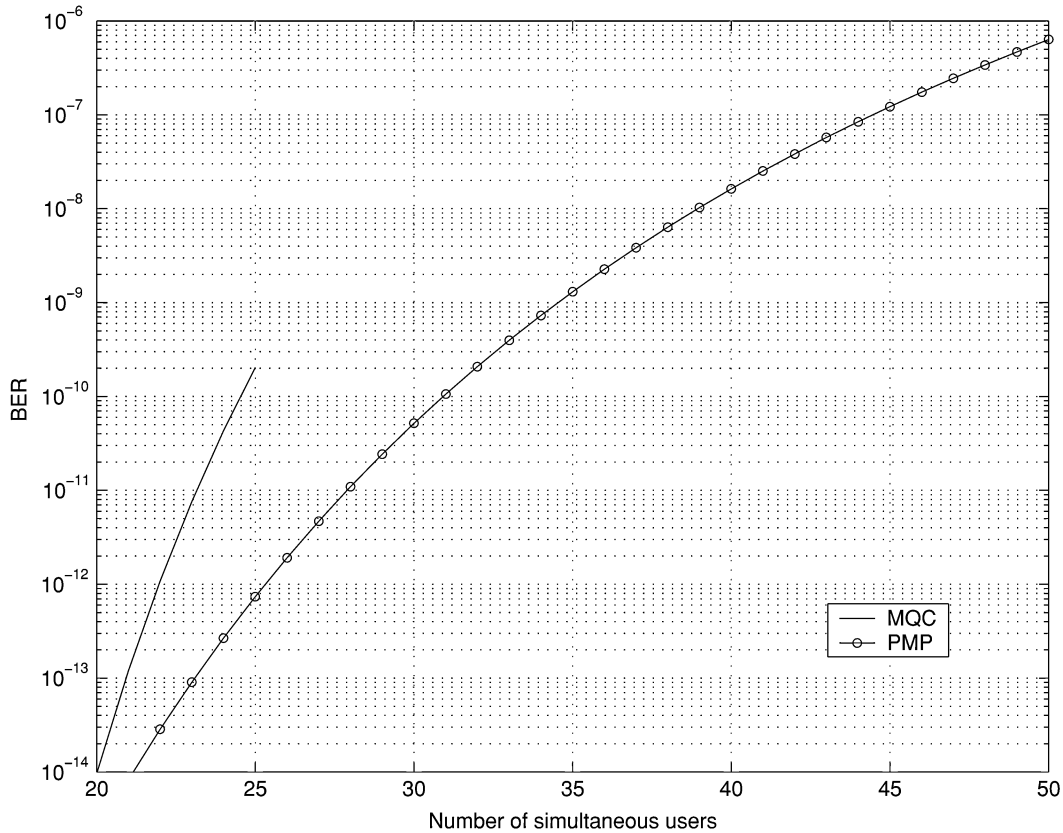


Fig. 5. The number of simultaneous users versus the BER for $p = 5$ with the effective source power equal to $-5$ dBm at a transmission rate of 622 Mb/s.

that the proposed system can employ the PMP codes with code length much shorter than that of to MQC codes to satisfy the requirement of EPON when transmission rate is 622 Mb/s and the effective source power is $-5$ dBm.

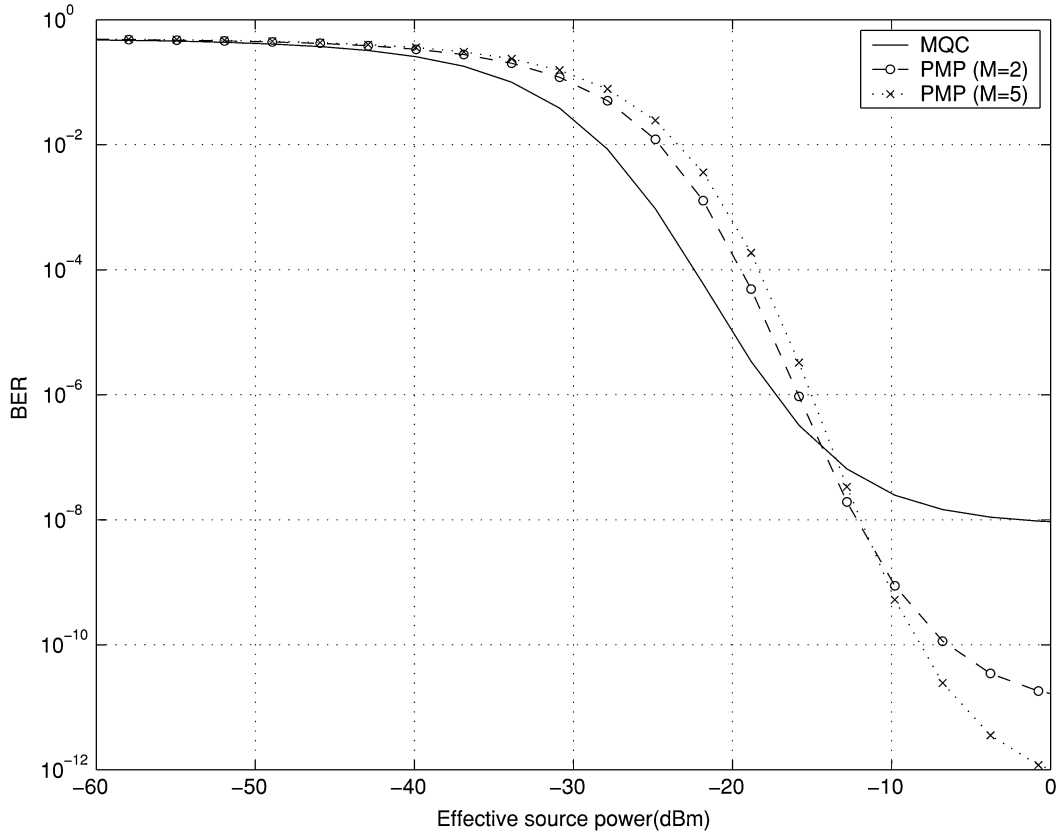


Fig. 6. The curves of effective source power versus the BER for the system using the PMP codes with $p = 11$ and $M = 2$ or 5 when number of simultaneous users is 85.

Fig. 6 shows the effective source power versus the BER for the system using the PMP codes with $p = 11$ and $M = 2$ or 5 when number of simultaneous users is 85. For comparison, the performance for the system using the MQC codes with $p = 11$ is also shown. As the figure shown, when the effective source power is sufficient, the system using PMP codes can reach better performance than the system using the MQC codes.

Besides, based on this numerical results, we find that the system performance increases with the value of $M$ provided that there is adequate effective source power at the receivers, because the beating probability of any two different code sequences of the PMP codes reduces when the value of $M$ increases and the PIIN can be further suppressed when the beating probability is lowered.

Therefore, in general, if the power of received signals is sufficient, the optimum value of $M$ is $(p-1)/2$, i.e., the largest factor of $(p-1)$ except for $(p-1)$ itself. However, if the power of received signals is insufficient, using large value of $M$ will make the proposed system susceptible to the shot noise and degrade the system performance. Hence, there is a tradeoff when choosing the value of $M$.

Fig. 7 shows theoretical estimations and the simulation results, which are acquired by using a software tool named "VPI-transmissionMaker", of the effective source power versus the BER for the system using PMP codes with $\mathrm{p} = 5$ and $\mathrm{M} = 2$. In the simulation, we use LEDs as the broadband sources and fiber Bragg gratings (FBGs) to implement the spectral encoders and decoders.

Since $\mathrm{p} = 5$ and $\mathrm{M} = 2$, the code weight of the used PMP codes is $(p-1)/M = 2$. Hence, each of the encoders and decoders is made to reflect two spectral components back and filter out others. In addition, each of the spectral components is set to have a bandwidth with 100 GHz. Thus, the effective bandwidth of the source is $\Delta f = p^2 \times 100$ GHz, i.e., 2.5 THz.

Besides, the differential path delay for the Mach–Zehnder interferometers is about several nanoseconds, the data rate is 155 Mb/s and the electrical bandwidth of the receivers is 80 MHz. The balanced detector consists of two APDs with quantum efficiency $\eta = 0.6$, average gain $G = 40$, excess noise factor $F_e \approx 21$ and effective ionization ratio $k_e = 0.5$.

In Fig. 7, the solid lines represent the theoretical estimations for $K = 1$ and $K = 9$, where $K$ represents the number of simultaneous users. The dashed lines represent the simulation results for $K = 1$ and $K = 9$, respectively. As shown in the figure, the theoretical estimations are quite close to the simulation results. The differences between the theoretical estimations and simulation results are smaller than 2 dB at $\mathrm{BER} = 10^{-9}$ for $K = 1$ and about 3 dB for $K = 9$.

The differences between the theoretical estimations and the simulation results are caused by various nonideal properties and power loss of the real-world optical components. For example, the FBGs are not able to filter out unmatched spectral components completely and will also cause power loss; the spectrum of the LEDs is not flat; the common-mode rejection ratio (CMRR) of the balanced detector is not infinite, etc.

## VI. Conclusion

In this paper, we present a family of new codes named PMP codes to lower the beating rate of any two different code se-

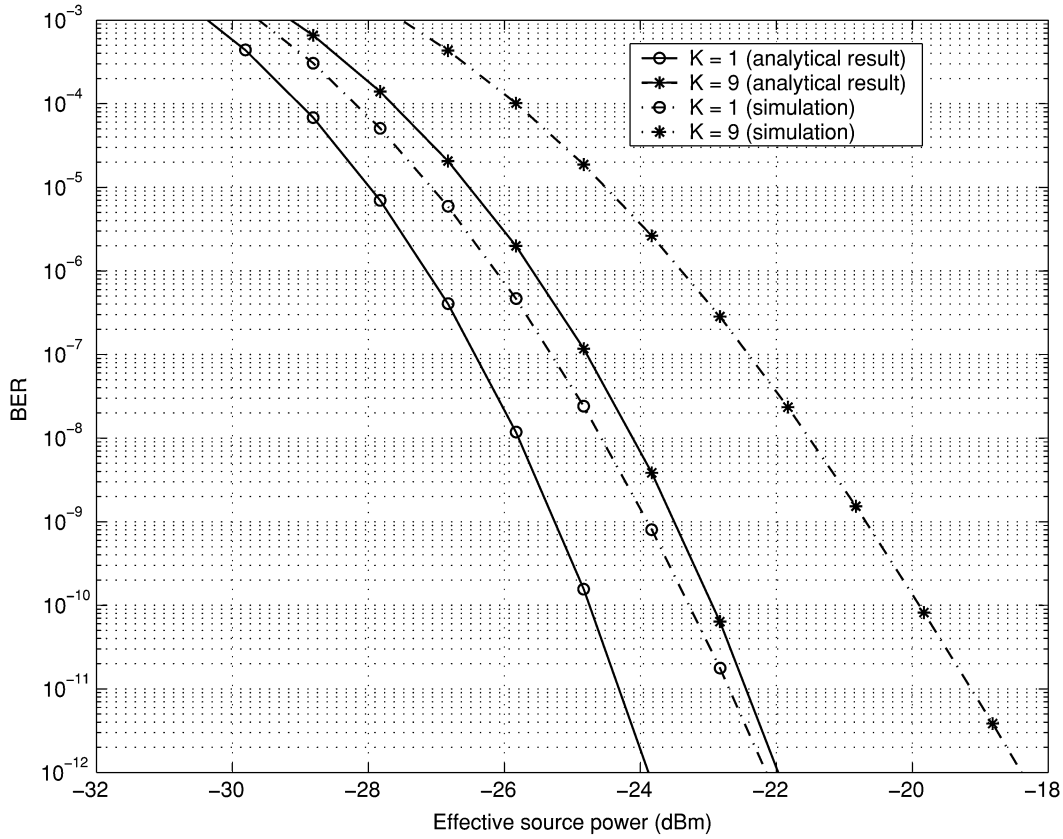


Fig. 7. The theoretical estimations and the simulation results of the effective source power versus the BER for the system using PMP codes with $\mathrm{p} = 5$ and $\mathrm{M} = 2$.

quences so as to suppress PIIN. The PMP codes are divided versions of the modified prime codes and hence have the value of in-phase cross-correlation not larger than one. We also propose a novel OCDMA system, which employs Mach–Zehnder interferometer pairs to eliminate the MUI and uses spectral encoders/decoders with PMP codes to suppress the PIIN. Since the beating rate can be reduced by increasing the value of the dividing factor $M$ of the PMP codes, the proposed system can effectively suppress PIIN. The codes size of the PMP codes can also be increased up to $M$ times as comparing with the modified prime codes. Hence, when the effective source power is adequate, the number of subscribers of the proposed system can be increased with the dividing factor $M$. Furthermore, the proposed system can also be applied to EPON. The results show that the proposed system can meet the EPON requirement at a transmission rate of 622 Mb/s by employing the PMP codes with code length much shorter than that of to MQC codes. In addition, the theoretical estimations of the proposed system are verified by the simulation results obtained via "VPItransmissionMaker" software tool.

## REFERENCES

[1] P. R. Prucnal, M. A. Santoro, and T. R. Fan, "Spread spectrum fiber-optic local area network using optical processing," *J. Lightw. Technol.*, vol. LT-4, pp. 547–554, May 1986.

[2] W. C. Kwong, P. A. Perrier, and P. R. Prucnal, "Performance comparison of asynchronous and synchronous code-division multiple-access techniques for fiber-optic local area networks," *IEEE Trans. Commun.*, vol. 39, pp. 1625–1634, Nov. 1991.

[3] C.-S. Weng and J. Wu, "Perfect difference codes for synchronous fiber-optic CDMA communication systems," *J. Lightw. Technol.*, vol. 19, pp. 186–194, Feb. 2001.

[4] J. A. Salehi, "Code division multiple-access techniques in optical fiber networks—Part I: Fundamental principles," *IEEE Trans. Commun.*, vol. 37, pp. 824–833, Aug. 1989.

[5] J. A. Salehi and C. A. Brackett, "Code division multiple-access techniques in optical fiber networks—Part II: System performance analysis," *IEEE Trans. Commun.*, vol. 37, pp. 834–842, Aug. 1989.

[6] F. R. K. Chung, J. A. Salehi, and V. K. Wei, "Optical orthogonal codes: Design, analysis, and applications," *IEEE Trans. Inform. Theory*, vol. 35, pp. 595–604, May 1989.

[7] M. Kavehrad and D. Zaccarin, "Optical code-division-multiplexed systems based on spectral encoding of noncoherent sources," *J. Lightw. Technol.*, vol. 13, no. 3, pp. 534–545, Mar. 1995.

[8] E. D. J. Smith, R. J. Blaikie, and D. P. Taylor, "Performance enhancement of spectral amplitude-coding optical CDMA using pulse-position modulation," *IEEE Trans. Commun.*, vol. 46, no. 3, pp. 1176–1185, Sep. 1998.

[9] X. Zhou, H. H. M. Shalaby, C. Lu, and T. Cheng, "Code for spectral amplitude coding optical CDMA systems," *Electronics Letters*, vol. 36, no. 8, pp. 728–729, Apr. 13th, 2000.

[10] Z. Wei, H. M. H. Shalaby, and H. Ghafouri-Shiraz, "Modified quadratic congruence codes for fiber Bragg-grating-based spectral-amplitude-coding optical CDMA systems," *J. Lightw. Technol.*, vol. 19, no. 9, pp. 1274–1281, Sept. 2001.

[11] G. J. Pendock and D. D. Sampson, "Capacity of coherence-multiplexed CDMA networks," *Optics Commun.*, vol. 143, no. 1–3, pp. 109–117, Nov. 1997.

[12] J. P. Goedgebuer, A. Hamel, H. Porte, and N. Butterlin, "Analysis of optical crosstalk in coherence multiplexed systems employing a short coherence laser diode with arbitrary power spectrum," *IEEE J. Quantum Electron.*, vol. 26, no. 7, pp. 1217–1226, Jul. 1990.

[13] A. Meijerink, G. H. L. M. Heideman, and W. C. van Etten, "A generalization of a coherence multiplexing system," in *Proc. 2000 Symposium on Communication and Vehicular Technology, SCVT-200*, vol. 19, Oct. 2000, pp. 6–13.

**Cheing-Hong Lin** was born in Taipei, Taiwan, R.O.C., in 1975. He received the B.S. degree in communication engineering from National Chiao Tung University, Hsinchu, Taiwan, R.O.C., and the M.S. degree in communication engineering from National Taiwan University, Taipei, Taiwan, R.O.C., in 1997 and 1999, respectively. He is currently pursuing the Ph.D. degree in communication engineering at the Fiber-Optic Communication Laboratory, National Taiwan University, Taipei, Taiwan.

His research interests include lightwave and wireless communication systems and computer networks.

**Jingshown Wu** (S'73–M'78–SM'99–F'03) received the B.S. and M.S. degrees in electrical engineering from National Taiwan University, Taipei, Taiwan, R.O.C., and the Ph.D. degree from Cornell University, Ithaca, NY, in 1970, 1972, and 1978, respectively.

He joined Bell Laboratories in 1978, where he worked on digital network standards and performance, and optical fiber communication systems. In 1984, he joined the Department of Electrical Engineering of National Taiwan University as Professor and was the Chairman from 1987 to 1989. He was also the Director of the Communication Research Center, College of Engineering of the university from 1992 to 1995. From 1995 to 1998, he was the Director of the Division of Engineering and Applied Science, National Science Council, R.O.C., on leave from the university. From 1999 and 2002, he was the Chairman of the Commission on Research and Development, and the Director of the Center for Sponsor Programs of National Taiwan University. Currently, he is the Vice-President of the university. He is interested in optical fiber communications, computer communications and communication systems. He has published more than 100 journal and conference papers and hold 11 patents.

Prof. Wu received the Distinguished Research Awards from National Science Council R.O.C. from 1991 to 1996 and the outstanding engineering professor award from the Chinese Institute of Engineers in 1996. He is a Life Member of the Chinese Institute of Engineers, the Optical Society of China, and the Institute of Chinese Electrical Engineers. He served as the Vice Chairman (1997–1998) and the Chairman (1998–2000) of IEEE Taipei Chapter.

**Hen-Wai Tsao** (S'77–M'90) received the B.S., M.S., and Ph.D. degrees in electrical engineering from the National Taiwan University, Taipei, Taiwan, R.O.C., in 1975, 1978, and 1990, respectively.

He joined the faculty of the Department of Electrical Engineering, National Taiwan University in 1978 and became Professor in 1991. His main area of interests is optical fiber communication system, communication electronics, and electronic instrumentation.

**Chun-Liang Yang** was born in I-Lan, Taiwan, R.O.C., in May 1971. He received the B.S., M.S., and Ph.D. degrees in electronic engineering from the National Taiwan University of Science and Technology (NTUST), Taiwan, R.O.C., in 1996, 1998, and 2004, respectively.

He is currently an Assistant Professor with the Department of Electrical Engineering, Tamkang University (TKU), Taipei, Taiwan, R.O.C. His research interests include optical performance monitoring and optical networks.